Correlation Between Computer Tomography-Derived Scar Topography and Critical Ablation Sites in Post-Infarction Ventricular Tachycardia

Michael Ghannam, MD, Hubert Cochet, MD§, Pierre Jais, MD§, Maxime Sermesant, PhD‡, Smita Patel, MD*, Konstantinos C. Siontis, MD, Fred Morady, MD, Frank Bogun, MD

Division of Cardiovascular Medicine, Department of Radiology*, University of Michigan, Ann Arbor, MI, USA
Bordeaux University Hospital and University of Bordeaux, Bordeaux, France§
INRIA, Sophia Antipolis, France‡

Address for correspondence:

Frank Bogun, MD
Cardiovascular Center, SPC 5853,
1500 East Medical Center Drive,
Ann Arbor, Michigan 48109-5853
Tel: 734 763 7141
Fax: 734 936 7026
E-mail: fbogun@med.umich.edu.

This research was supported by funding from the French National Research Agency (ANR) under Grant Agreements Equipex MUSIC ANR-11-EQPX-0030, IHU LIRYC ANR-10-IAHU-04, and MIGAT ANR-13-PRTS-0014-01.

Disclosures: None

Background: Myocardial wall thickness (WT) in patients with a prior myocardial infarction has been used to indicate scarring. However, the correlation of WT with sites critical to ventricular tachycardia (VT) has not been previously investigated. The purpose of this study was to correlate electroanatomic mapping data obtained during VT ablation with WT determined by cardiac computed tomography (CT).

Methods and Results: Cardiac CTs were performed in 15 consecutive patients (mean age 63±10 years, 86% male, left ventricular ejection fraction 27±12%) with a prior infarct referred for VT ablation. The CTs were registered to the electroanatomic maps obtained during the mapping procedure. Pacing was performed throughout the scar at sites with fractionated electrograms and isolated potentials. Ablation sites were identified by pace-mapping or entrainment-mapping and these sites were correlated with WT. Bipolar and unipolar voltage amplitude and bipolar electrogram width correlated with WT (correlation coefficient: 0.63, 0.65 and 0.41, respectively, $p<0.001$). Ablation target sites were identified for 58/113 inducible VTs. The ablation target sites were located on CT- defined ridges (WT: 4.2±1.2 mm) bordered by areas of thinning (WT: 2.6±1.1 mm, $p<0.0001$) in 14/15 patients. Ablation targets were found on ridges in 49/58 VTs (84%) for which target sites were identified. A total of 70 ridges were localized in the 15 patients. VT became non-inducible post-ablation in 11/15 patients (73%).

Conclusion: WT measured by CT identifies ridges of myocardial tissue that often are critical for post-infarction VT and that can be appropriate target sites for ablation.

Various imaging techniques have been employed to identify the scar and the arrhythmogenic substrate in order to facilitate procedural planning and execution[1]. Magnetic resonance imaging is the gold-standard for identifying myocardial scar[2], but has spatial resolution limitations and is often not feasible in patients with an implanted cardioverter defibrillator (ICD). Multi-detector computed tomography (CT) can be used safely in patients with implanted devices and has the benefit of rapid acquisition times and superior spatial resolution. CT can provide detailed anatomic information as well as information on myocardial function, perfusion, and viability, and has been shown to correlate well with MRI-defined scar locations[3-5]. Prior investigations into the use of CT to aide in VT ablations have focused on using a wall thickness cut-off value of <5 mm to delineate healthy from scarred myocardium[4]. The correlation between wall thickness and the arrhythmogenic substrate and electrophysiologic parameters within scar has not been systematically been performed. The purpose of this study was to correlate wall thickness as assessed by cardiac CT with the arrhythmogenic substrate and mapping data in post-infarction VT.

Methods

Patient Characteristics (Table 1)

The subjects of this study were 15 consecutive patients (mean age 63±10 years, 86% male, left ventricular ejection fraction 27±12%) with recurrent post-infarction VT who underwent catheter ablation in the left ventricle. The patients were consecutive in that they had no contraindications for CT scanning. All patients had an ICD and 4 patients had undergone prior ablation procedures. At the time of the procedure, 14 patients were taking antiarrhythmic medications, including amiodarone in 9 patients.

Computed Tomography Acquisition and Processing

Contrast-enhanced ECG-Gated CT of the heart was performed on the GE Discovery HD-750, 64-slice CT scanner (GE Healthcare, Milwaukee, WI) 1 to 3 days before the ablation procedure. Images were acquired during an inspiratory breath-hold with prospective/retrospective gating dependent on heart rate and variability. Following a timing bolus of 15 mL/s, a dedicated ECG-gated CT angiographic acquisition was obtained with a 3 phase injection of a total of 100 mL of iodinated contrast agent Iopamidol 370, and 50 mL of Saline (Isovue 370) (Bracco Diagnostics Inc., New Jersey) at a rate of 5 mL/s. To maximize the contrast on both sides of the septum, a dedicated injection protocol was applied, in order to obtain homogeneous enhancement of left and right chambers. Acquisition parameters were slice thickness, 0.625 mm; tube voltage, 100-120 kVp and variable mA dependent on patient BMI; and gantry rotation time, 350 ms. Image processing was performed as previously described[4] using proprietary software (MUSIC software, IHU LIRYC Bordeaux and Inria Sophia Antipolis, France)[6, 7]. Briefly, the epicardium was manually contoured around the left ventricular (LV)-free wall and the right side of the interventricular septum on short axis images. The endocardium and coronary vessels were segmented using automated region growing segmentation and automated vessel analysis. Wall thickness values were automatically derived from endo- and epicardial contours.

Areas of wall thickness less than 5 mm were identified as abnormal based on reports of CT derived wall thickness in healthy patients[8]. Areas of wall thickness of ≤5 mm, ≤4mm, ≤3mm, ≤2mm, and ≤1mm were created for our analysis (Figure 1).

Electrophysiology Study and Mapping Protocol

The study protocol was approved by the Human Research Committee. After informed consent was obtained, multielectrode catheters were positioned in the high right atrium, the His position and the right ventricular apex. Programmed right ventricular stimulation was performed in all patients with up to four extrastimuli from two right ventricular sites until refractoriness or a coupling interval of 200 msec was reached. Completion of the protocol was attempted in patients who were hemodynamically stable. A maximum of 5 cardioversions were performed as necessary. The same stimulation protocol was repeated after the ablation procedure. VTs were defined as separate morphologies provided that the QRS complex differed in ≥3 leads from each other.

The mapping protocol has been previously described[9]. Electroanatomical mapping (CARTO, Biosense Webster, Diamond Bar, CA) was performed with a 3.5-mm-tip, open-irrigation ablation catheter (Thermocool). Electrograms were filtered at 50–500 Hz. The intracardiac electrograms and leads V1, I, II, and III were displayed on an oscilloscope and recorded at a speed of 100 mm/s. The recordings were stored on optical disc (St. Jude Medical, St. Paul, MN, USA). Low voltage was defined as a bipolar voltage amplitude ≤ 1.5 mV. Dense scar was defined by a bipolar voltage amplitude <0.5 mV[10]. A mean of 998±274 points (range: 666-1404) per patient were obtained to generate the voltage map. For tolerated VTs, entrainment mapping was used to identify target sites. For non-tolerated VTs, pace-mapping was performed to identify target sites. These target sites were correlated *post hoc* with areas of wall thinning identified by CT (Figure 2, 3). A pace-map was considered to match the targeted VT morphology if ≥10/12 leads of the pace-map matched with the QRS morphology of the induced VT. Pace-maps meeting a more strict criteria of 12/12 matching leads were also identified for separate analysis. For multiple sites with matching pace-maps,

sites were defined as distinct if they were at least 5 mm apart. The stimulus-QRS interval at sites with matching pace-maps was measured and correlated with the location within the scar. A stimulus-QRS/VT cycle length ratio ≤0.3 was considered a short interval indicating a VT exit and a stimulus-QRS/VT cycle length ratio >0.3 was defined as a long interval.

Radiofrequency Ablation

If the VT was hemodynamically tolerated, entrainment mapping was performed and radiofrequency energy was delivered at sites with concealed entrainment. In the case of hemodynamically unstable VT, ablation was performed during sinus rhythm at sites with matching pace-maps or sites with fragmented or isolated electrograms. Radiofrequency energy was delivered for 60-120 seconds in an attempt to render the ablated site unexcitable with a pacing output of 20 mA using an initial power of 30 Watts that was titrated upwards to 50 watts as necessary. Post-ablation, programmed ventricular stimulation was repeated using the same stimulation protocol.

Three-Dimensional Registration

For 3D registration of electroanatomical geometry with the CT model, three identifiable anatomic reference points (coronary sinus ostium, ostium of the left main coronary artery as defined by intracardiac ultrasound, and left ventricular apex) were used for alignment and orientation. After initial alignment using fixed landmarks, automatic surface registration using CartoMerge (Biosense Webster) was performed as previously described[11]. CT-derived wall thickness was represented as separate shells (≤1mm, ≤2 mm, ≤3 mm, ≤4 mm, and ≤5 mm, Figure 1) that were co-registered with the electroanatomic map using 3 fiducial

anatomic points. The wall thickness shells were registered to the electroanatomic map post hoc after the ablation procedure. This was done by an operator blinded to the outcome of the ablation procedure. The CT was registered to the electroanatomic maps with a positional error of 2.9±2.2 mm. The areas of low voltage and dense scar were measured and correlated to the areas of wall thinning ≤ 1mm, ≤2 mm, ≤3 mm, ≤4 mm and ≤5 mm.

Data Acquisition and Analysis

In a *post hoc* analysis, the following variables were acquired at 1379 sites (mean of 92±25 sites per patient) where pace-mapping was performed and were correlated with wall thickness: bipolar voltage, unipolar voltage, electrogram characteristics (normal, abnormal, fragmented, isolated potentials), electrogram width, presence of a matching pace-map, and presence of concealed entrainment. Electrograms were classified according to previously reported criteria[12] that were adapted[13] to the recording system used in this study: The following criteria were used: normal electrograms- sharp biphasic or triphasic spikes with amplitudes 3 mV, duration 70 ms, and/or amplitude:duration ratio 0.046; fractionated electrograms- amplitude 0.5 mV, duration 133 ms, and/or amplitude:duration ratio 0.005.; isolated potential- a potential separated from the ventricular electrogram by an isoelectric segment and/or a segment with low-amplitude noise (0.05 mV) of 20 ms duration at a gain of 40–80 mm/mV; the remaining electrograms were classified as abnormal.

The scar area and the surface area of the different wall thickness segments were measured using the CARTO 3 software and correlated with each other. Borderzone sites (0.5-1.5 mV) were analyzed for wall thickness and categorized into sites with matching and sites without matching pace-maps. The locations of target sites were identified and correlated with wall thickness (Figure 1). Scar was defined on CT as areas with thickness <5 mm. Within this

CT-scar area, ridges were defined as areas that showed a wall thickness exceeding the surrounding wall thickness by at least 1 mm, and that had the shape of a channel. By merging different layers of wall-thickness over each other, ridges were identified where thicker areas (difference ≥1 mm) were embedded in thinner areas (Figure 1). The area of ridges was measured by subtracting areas of thinning from the superimposed thicker wall segments. The overlay resulting in the largest number of ridges was chosen as the topographic CT structure to correlate with mapping defined target sites (Figure 2). This approach was chosen in order not to miss areas that may be critical for VT. Two operators blinded to the procedural outcome analyzed location and number of ridges. Discrepancies were resolved by consensus. Figure 1 illustrates the topographic map correlated with the electroanatomic map of a patient indicating an isthmus critical to VT. Figure 4 shows a VT isthmus corresponding with a CT defined ridge.

After the electroanatomic map was constructed, bipolar voltage-derived channels were sought as previously described and correlated with the presence of CT-defined ridges and ablation target sites[14]. This analysis was performed by 2 observers blinded to the procedure outcome. Discrepancies were resolved by consensus. In brief, the cut-off bipolar voltage within the voltage map was set to 0.2 mV in order to identify a corridor of more preserved voltage[14]. If an area of more preserved voltage was identified this was correlated with the CT-defined ridges with respect to orientation and also whether or not the voltage derived channels contained mapping derived target sites.

Statistical Analysis

Continuous variables were expressed as mean ± standard deviations for normally distributed data and compared using the Student's T-test, while non-normally distributed data

were expressed as median and interquartile ranges (IQR) and were compared using the Mann-Whitney U test. Categorical data were compared using χ^2 or Fisher's exact test, as appropriate. Spearman rho correlation coefficients were generated to examine the relationship between myocardial wall thickness and EGM properties. Receiver operator characteristic curves (ROC) were created using myocardial wall thickness to assess the ability of different myocardial wall thickness cutoffs to predict scar tissue (bipolar amplitude <1.5mV), dense scar tissue (bipolar amplitude <0.5mV) and mapping defined target site locations. All tests were two tailed and a P value <0.05 was considered significant. Statistical analysis was performed using R version 3.3.1 (R foundation, Vienna, Austria) and IBM SPSS Statistics software version 24 (IBM).

Results

Procedural Characteristics

A total of 113 VTs with a mean cycle length of 375±112 ms were inducible (7.5±4.3 VTs per patient). Forty-seven VTs had a left bundle branch block and 66 VTs had a right bundle branch block morphology. Ten patients did not have a hemodynamically-tolerated VT and ablation was guided by pace mapping and electrogram characteristics (fragmentation, isolated diastolic potentials). Entrainment mapping was feasible in 5 patients. Eleven of these 15 patients no longer had inducible VT post-ablation. In the other 4 patients the clinical VTs were eliminated but 6 non-clinical VTs (cycle length: 338±99 msec) remained inducible. In one patient programmed stimulation was not repeated at the conclusion of the procedure due to a possible thromboembolic event. This was subsequently ruled out. There were no major complications.

Characterization of the Arrhythmogenic Substrate and Wall Thickness

A total of 202 target sites were identified by pace-mapping (n=191) and entrainment mapping (n=11) and were correlated with wall thickness (Figure 2). There were no significant differences between target sites and non-target sites in median bipolar voltage, bipolar EGM width, or unipolar voltages ($p>0.05$ for all). The relationship of target sites to wall thickness is shown in Figure 2. Target sites (n=202) did not differ in wall thickness from non-target sites (n=1175; 3.4±1.7 vs 3.5±1.7 mm, p=0.88). They had a mean voltage of 1.01±1.3 mV, were more often located at sites with preserved voltage (>0.5 mV: 55%) compared to sites with dense scar (≤0.5 mV: 45%). They consisted most often of exit sites (82%) vs non-exit sites (18%).

VT target sites in 14/15 patients were located on a ridge of tissue (mean thickness 4.2±1.2 mm) bounded by areas of wall thinning (mean thickness 2.6±1.1 mm [$p<0.0001$]). In the remaining 1/15 patients target sites were located on an area of thinning bordered by normal voltage tissue.

In 49/58 VTs (84%) for which target sites were identified, the sites were located on ridges bordered by areas of thinning (n=33), or between areas of thinning and anatomical barriers (n=6), or on a ridge merging with an area of normal thickness with the ridge extending out from the scar (n=10). For the remaining 9 VTs, target sites were located on a segment of thinning facing an area of normal thickness (n=8) or located on a papillary muscle (n=1).

A total of 70 ridges were identified in the 15 patients (mean 4.7±3.3 ridges per patient). A target site for ablation was identified on 35 of the 70 ridges (mean of 2.0±1.8 ridges per patient). The mean minimum width of the ridges was 8.4±6.7mm.

The ridges of thicker tissue traversed the entire scar in 11/15 patients. In 9/15 patients, multiple target sites with long and short stimulus/QRS intervals were identified along these ridges for a total of 16 VTs. Sites with long stimulus-QRS intervals were located further within the scar (a mean of 25.5±13 mm from tissue with normal voltage) compared to target sites with short stimulus-QRS intervals (a mean of 11±11 mm from tissue with normal voltage, $p<0.0001$) that were located in or close to the border zone. In 5/15 patients, mapping was performed during VT and in all 8/8 sites that demonstrated concealed entrainment and VT termination during ablation, the sites were located on a ridge bordered by 2 areas of thinning (Figure 1). All VTs with sites demonstrating either concealed entrainment or matching pace-maps were rendered non-inducible post ablation in patients in whom programmed stimulation was performed post ablation (n=14).

At target sites, the stimulus-QRS/VT cycle length ratios were compared across the different myocardial wall thicknesses (Table 2). There was a modest inverse correlation between the degree of wall thinning and the stimulus-QRS/VT cycle length ratio (correlation coefficient -0.54, $p<0.001$).

The majority of the target sites 158/202 (78%) were located on a ridge with a distance of 4.8±3.0 mm from an area of wall thinning. Remaining target sites were located on the thinnest wall segments (n=29, 14%) or along thin wall segments bordered by normal tissue (n=15, 7%)

Electroanatomic Map and Wall Thinning

A wall thickness cut-off ≤ 4 mm was 86% sensitive and 78% specific for detecting a voltage cut-off <1.5 mV (AUC= 0.83, p<0.001). A wall thickness cut-off ≤ 3 mm was 90% sensitive and 55% specific for detecting a voltage cut-off <0.5 mV (AUC= 0.78, p<0.001).

The median low voltage area (<1.5 mV) was 120 cm^2 [IQR: 77-165 cm^2] compared to a wall thinning area <5 mm of 150 cm^2 [IQR: 94 -194 cm^2]. The median area of the CT defined ridges was 38 cm^2 [IQR: 21-88 cm^2]. The ridge area was on average 37±15% the area of the low voltage bipolar map value (p<0.05).

A total of 21 voltage-derived channels were identified in 14 of the 15 patients. Nine of 70 ridges correlated with a channel identified by voltage mapping and the voltage derived channels contained target sites for 10/58 VTs.

Electrogram Characteristics and Wall Thinning

The characteristics of electrograms at various wall thicknesses are displayed in Table 2 and 3. Bipolar electrogram voltage amplitude, unipolar voltage amplitude, and bipolar electrogram width were all moderately correlated with wall thickness (correlation coefficients of 0.63, 0.65 and 0.45, respectively, p<0.001 for all), with thinner myocardium displaying lower bipolar/unipolar amplitude and wider bipolar EMGs. Electrograms characterized as abnormal or fractionated and those with isolated potentials were more likely to be found in areas of myocardium with thin wall segments (Table 3, p<0.001 for all).

Follow-up

Antiarrhythmic medications were discontinued in 5 patients after the ablation procedure. Over a follow-up period of 4.24±2.6 months one patient had recurrent VT.

Discussion

Main Findings

Local differences in wall thickness reflect the arrhythmogenic structure of the post-infarction scar in patients with VT. Effective VT ablation sites were located on ridges within the scar bordered by areas of wall thinning for the majority of mapped VTs in the present study. Electroanatomic mapping data correlated with wall thinning. Wall thinning measured by CT is a promising imaging technique that may help to improve the characterization of the arrhythmogenic scar in post-infarction patients and assist in identifying effective target sites for ablation of VT.

Imaging of the Arrhythmogenic Substrate

Scar identified by delayed enhanced magnetic resonance imaging has been the gold standard for scar identification in patients with prior infarctions[2] and has been used to identify the arrhythmogenic substrate in patients with prior infarctions[15]. Myocardial fiber bundles can by identified by high resolution ex-vivo MRI[16]. However, when retrospective degradation of the magnetic resonance images was used to obtain a resolution comparable to that of clinical scans, areas of intermediate signal intensity were often attributed to the phenomenon of partial volume averaging and not surviving myofiber bundles within scar tissue[16].

On the other hand, using different threshold techniques for scar analysis, the grey zone has been described as an indicator of tissue heterogeneity within scar tissue[17]. Perez-David, et al correlated conducting channels critical for VT with signal heterogeneity as determined by MRI[18]. However, another study did not demonstrate an association between the signal intensity of delayed enhanced areas and critical sites of the reentry circuit[15]. Furthermore, scar imaging is challenging, especially in patients with implanted devices and alternative imaging techniques are needed. Unfortunately, in patients with implanted devices, artifacts render the imaging quality suboptimal to allow for more precise targeting based on the MR images alone. The present study demonstrates that scar heterogeneity as determined by CT can identify the arrhythmogenic substrate in consecutive patients with post-infarction VT. The advantages of CT over MRI are more widespread availability, superior spatial resolution, and precise threshold definition resulting in the ability to accurately identify critical sites within a VT reentry circuit. The rationale for using wall thickness to characterize scar heterogeneity is the hypothesis that surviving fibers within scar, that is the structural substrate of scar-related VT, are more likely to be observed in areas of relatively preserved thickness than in extremely thinned areas where scar is expected to be more dense. The use of CT to measure wall thickness is justified by the unique 3-dimensional spatial resolution of the method, and by its excellent contrast to delineate endocardial and epicardial surfaces. Our results demonstrating a clustering of target sites on ridges of relatively preserved thickness bordered by more severely thinned areas can be viewed as a first proof of concept substantiating our hypothesis.

Scar Topography and Reentry Circuits

CT reveals a view of an infarct area that is different than that provided by late gadolinium enhanced-MRI. The infarcted myocardium has ridges and sinks that may determine the location of reentry circuits. In most patients in this series, ablation target sites were located on ridges that divided areas of wall thinning. These ridges can travel through the entire scar and divide the scar into different zones of thinner and thicker wall segments. Matching pace-maps with shorter and longer stimulus-QRS intervals were observed along these ridges, suggesting a link between impulse propagation and CT-defined structure. The ridges where effective ablation sites were found were most often located in the border zone of the scar. However, some of the ridges containing target sites were not near the border zone. Based on the correlation between the mapping data and locations of effective ablation sites, the results of this study indicate that the CT-defined ridges often are critical anatomic components of post-infarction VT reentry circuits.

Voltage defined channels described by others[14] were found in most patients. However, they only occasionally corresponded to an anatomic ridge and identified an ablation target site for only a minority of VTs. This indicates that anatomic ridges may be more accurate than voltage defined channels for identifying a critical component of the post-infarction VT reentry circuit. Furthermore, it may be surprising that segments with the thinnest diameter contained the broadest and most abnormal electrograms. Yet the thicker segments contained the targeted ablation sites. This is due to the fact that the majority of the target sites were exit sites that were located in areas with thicker segments located close to normal myocardial tissue.

Wall Thinning and Electroanatomic Mapping

Wall thickness measured by CT correlated with voltage data generated during electroanatomical mapping, and electrogram characteristics including bipolar voltage and electrogram width also correlated well with wall thickness. Location of borderzone and dense scarring can therefore be determined by imaging well before the ablation procedure. Furthermore, imaging provides more localizing information regarding critical ablation areas over electroanatomic mapping.

Limitations

The main limitation is the absence of a control group of patients with a prior infarction but without ventricular tachycardia. In the absence of this type of control group, the specificity of anatomic ridges for critical sites in a ventricular tachycardia reentry circuit remains unclear. A simple algorithm to determine differences in wall thickness was used, and on these maps ridges were assessed visually. This algorithm should be further optimized to enable automated ridge detection, and its ability to predict reentry circuits should be assessed in a larger patient population. Further improvement of the algorithm may also improve the specificity for CT defined ridges to identify critical VT sites. Ablation target sites were defined by pace-mapping and entrainment mapping. We acknowledge that pace-mapping-defined target sites are less specific and may be the consequence of blind loops of the reentry circuit. However, the fact that none of the VTs with matching pace-maps could be induced post ablation indicates that these sites likely were critical for the targeted VTs. In the absence of matching pace-maps, radiofrequency energy was also delivered at sites with fragmented electrograms and thereby may have eliminated VTs without identifiable exit sites. Whether an ablation using a purely "ridge-defined" strategy will generate similar ablation results remains to be determined.

Conclusions

CT-derived wall thickness of post-infarction scar indicates areas that may be critical for post-infarction VT. Thicker ridges within areas of pronounced wall thinning appear to indicate the imaging equivalent of the critical arrhythmogenic substrate in post-infarction VT.

Acknowledgement: We would like to thank Melissa A. Muck, R.T. (R)(CT) for her help with CT image acquisition and image processing.

References:

1. Njeim M, Desjardins B, Bogun F. Multimodality imaging for guiding ep ablation procedures. *JACC Cardiovasc Imaging*. 2016;9:873-886
2. Kim RJ, Fieno DS, Parrish TB, Harris K, Chen EL, Simonetti O, Bundy J, Finn JP, Klocke FJ, Judd RM. Relationship of mri delayed contrast enhancement to irreversible injury, infarct age, and contractile function. *Circulation*. 1999;100:1992-2002
3. Tian J, Jeudy J, Smith MF, Jimenez A, Yin X, Bruce PA, Lei P, Turgeman A, Abbo A, Shekhar R, Saba M, Shorofsky S, Dickfeld T. Three-dimensional contrast-enhanced multidetector ct for anatomic, dynamic, and perfusion characterization of abnormal myocardium to guide ventricular tachycardia ablations. *Circ Arrhythm Electrophysiol*. 2010;3:496-504
4. Komatsu Y, Cochet H, Jadidi A, Sacher F, Shah A, Derval N, Scherr D, Pascale P, Roten L, Denis A, Ramoul K, Miyazaki S, Daly M, Riffaud M, Sermesant M, Relan J, Ayache N, Kim S, Montaudon M, Laurent F, Hocini M, Haissaguerre M, Jais P. Regional myocardial wall thinning at multidetector computed tomography correlates to arrhythmogenic substrate in postinfarction ventricular tachycardia: Assessment of structural and electrical substrate. *Circ Arrhythm Electrophysiol*. 2013;6:342-350
5. Esposito A, Palmisano A, Antunes S, Maccabelli G, Colantoni C, Rancoita PM, Baratto F, Di Serio C, Rizzo G, De Cobelli F, Della Bella P, Del Maschio A. Cardiac ct with delayed enhancement in the characterization of ventricular tachycardia structural substrate: Relationship between ct-segmented scar and electro-anatomic mapping. *JACC Cardiovasc Imaging*. 2016;9:822-832
6. Cochet H, Dubois R, Sacher F, Derval N, Sermesant M, Hocini M, Montaudon M, Haissaguerre M, Laurent F, Jais P. Cardiac arrythmias: Multimodal assessment integrating body surface ecg mapping into cardiac imaging. *Radiology*. 2014;271:239-247
7. Yamashita S, Sacher F, Mahida S, Berte B, Lim HS, Komatsu Y, Amraoui S, Denis A, Derval N, Laurent F, Sermesant M, Montaudon M, Hocini M, Haissaguerre M, Jais P, Cochet H. Image integration to guide catheter ablation in scar-related ventricular tachycardia. *J Cardiovasc Electrophysiol*. 2016;27:699-708
8. Stolzmann P, Scheffel H, Leschka S, Schertler T, Frauenfelder T, Kaufmann PA, Marincek B, Alkadhi H. Reference values for quantitative left ventricular and left atrial measurements in cardiac computed tomography. *Eur Radiol*. 2008;18:1625-1634
9. Bogun F, Good E, Reich S, Elmouchi D, Igic P, Lemola K, Tschopp D, Jongnarangsin K, Oral H, Chugh A, Pelosi F, Morady F. Isolated potentials during sinus rhythm and pace-mapping within scars as guides for ablation of post-infarction ventricular tachycardia. *J Am Coll Cardiol*. 2006;47:2013-2019
10. Marchlinski FE, Callans DJ, Gottlieb CD, Zado E. Linear ablation lesions for control of unmappable ventricular tachycardia in patients with ischemic and nonischemic cardiomyopathy. *Circulation*. 2000;101:1288-1296
11. Wijnmaalen AP, van der Geest RJ, van Huls van Taxis CF, Siebelink HM, Kroft LJ, Bax JJ, Reiber JH, Schalij MJ, Zeppenfeld K. Head-to-head comparison of contrast-enhanced magnetic resonance imaging and electroanatomical voltage mapping to assess post-infarct scar characteristics in patients with ventricular tachycardias: Real-time image integration and reversed registration. *European heart journal*. 2011;32:104-114
12. Josephson M. *Clinical cardiac electrophysiology techniques and interpretations*. Lea & Febiger; 1993.
13. Bogun F, Good E, Reich S, Elmouchi D, Igic P, Lemola K, Tschopp D, Oral H, Chugh A, Pelosi F, Morady F. Isolated potentials during sinus rhythm and pace-mapping within scars as guides for ablation of post-infarction ventricular tachycardia. *Journal of the American College of Cardiology*. 2006;47:2013-2019

14. Arenal A, del Castillo S, Gonzalez-Torrecilla E, Atienza F, Ortiz M, Jimenez J, Puchol A, Garcia J, Almendral J. Tachycardia-related channel in the scar tissue in patients with sustained monomorphic ventricular tachycardias: Influence of the voltage scar definition. *Circulation*. 2004;110:2568-2574
15. Desjardins B, Crawford T, Good E, Oral H, Chugh A, Pelosi F, Morady F, Bogun F. Infarct architecture and characteristics on delayed enhanced magnetic resonance imaging and electroanatomic mapping in patients with postinfarction ventricular arrhythmia. *Heart Rhythm*. 2009;6:644-651
16. Schelbert EB, Hsu LY, Anderson SA, Mohanty BD, Karim SM, Kellman P, Aletras AH, Arai AE. Late gadolinium-enhancement cardiac magnetic resonance identifies postinfarction myocardial fibrosis and the border zone at the near cellular level in ex vivo rat heart. *Circ Cardiovasc Imaging*. 2010;3:743-752
17. Schmidt A, Azevedo CF, Cheng A, Gupta SN, Bluemke DA, Foo TK, Gerstenblith G, Weiss RG, Marban E, Tomaselli GF, Lima JA, Wu KC. Infarct tissue heterogeneity by magnetic resonance imaging identifies enhanced cardiac arrhythmia susceptibility in patients with left ventricular dysfunction. *Circulation*. 2007
18. Perez-David E, Arenal A, Rubio-Guivernau JL, del Castillo R, Atea L, Arbelo E, Caballero E, Celorrio V, Datino T, Gonzalez-Torrecilla E, Atienza F, Ledesma-Carbayo MJ, Bermejo J, Medina A, Fernandez-Aviles F. Noninvasive identification of ventricular tachycardia-related conducting channels using contrast-enhanced magnetic resonance imaging in patients with chronic myocardial infarction: Comparison of signal intensity scar mapping and endocardial voltage mapping. *Journal of the American College of Cardiology*. 2011;57:184-194

Table 1: Patient Characteristics

Patients	Age	Gender	EF (%)	#induced VTs prior RF	# induced VTs post RF
1	48	Male	30	8	1
2	62	Male	25	9	0
3	73	Male	38	1	0
4	72	Male	30	2	1
5	41	Female	25	14	0
6	78	Male	55	9	0
7	67	Male	45	6	0
8	65	Male	35	14	3
9	68	Male	15	4	0
10	67	Male	15	5	0
11	68	Female	15	1	0
12	64	Male	25	12	1
13	60	Male	15	11	NA
14	51	Male	15	8	0
15	63	Male	25	9	0

Abbreviations: EF=ejection fraction, ind VTs prior RF= induced VTs prior to radiofrequency ablation,

Table 2: Correlation of Wall Thickness and Electroanatomic Mapping Characteristics

Wall Thickness	Bipolar Voltage (mV)	Unipolar Voltage (mV)	EGM width (msec)	S-QRS interval /VT cycle length	Total #
≤1 mm	0.21 [.10 - 0.30]	2.0 [1.43 – 2.65]	184 [153 – 204]	0.31 [0.18 – 0.38]	167
≤2 mm	0.35 [0.20 - 0.58]	2.77 [2.08 – 3.69]	148 [133 – 170]	0.21 [0.10 – 0.33]	276
≤3 mm	0.53 [0.34 – 0.80]	2.88 [2.16 - 3.66]	139 [117 – 158]	0.22 [0.17 – 0.32]	371
≤4 mm	0.68 [0.44 – 1.13]	3.44 [2.44 – 4.66]	125 [101 – 138]	0.12 [0.08 – 0.16]	150
≤5 mm	0.94 [0.58 – 1.53]	4.38 [2.85 – 5.80]	111 [91 – 131]	0.11 [0.08 – 0.13]	157
>5 mm	1.39 [0.70 – 2.99]	5.32 [3.10 – 8.06]	90 [70 – 112]	0.09 [0.06 – 0.12]	259

Values are shown as median (IQR).

Abbreviations: EGM= electrogram, S-QRS interval= stimulus-QRS interval

Table 3: Electrogram Characteristics depending on Wall Thickness

Wall Thickness	Normal EGM	Fractionated EGM	Isolated Potentials	Abnormal EGM	Total # of EGMs
≤1 mm	0.00%	73.05%	9.58%	17.96%	167
≤2 mm	0.36%	44.00%	5.09%	49.82%	275
≤3 mm	0.27%	27.22%	2.16%	69.27%	371
≤4 mm	0.67%	16.11%	1.34%	82.55%	149
≤5 mm	0.64%	9.62%	0.00%	89.74%	159
>5 mm	22.78%	4.63%	0.00%	71.43%	259

Abbreviations: as above.

Figure Legends:

Figure 1

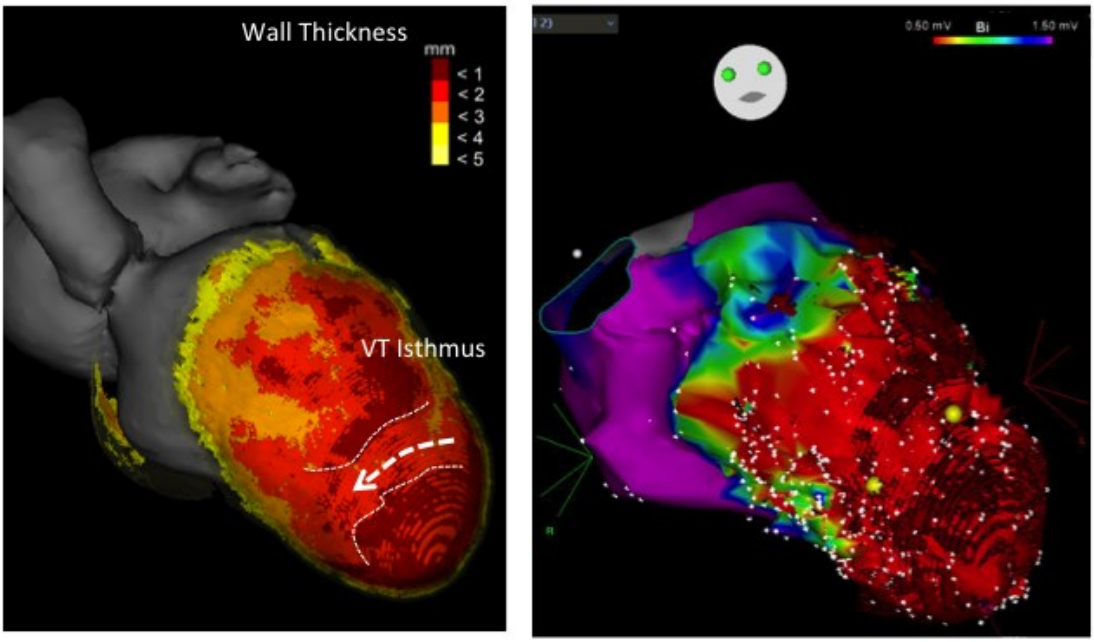

Figure 1: Left Panel: Wall thickness as determined by CT. Shown is the anteroseptal aspect of the left ventricle from a patient with a prior anterior wall myocardial infarction. The wall thickness is color coded. A VT isthmus is indicated in the anteroapical free wall. The isthmus is located between 2 distinct areas of thinning (<1 mm in wall thickness) between the apex and the mid anterior left ventricle (white lines and arrow).

Right Panel: The shell of the CT defined wall thinning is registered to the bipolar electroanatomic voltage map. Two sites (yellow tags) indicate sites were pacing was performed during VT indicating sites with concealed entrainment and matching stimulus-QRS and electrogram QRS intervals where VT terminated during ablation.

Figure 2

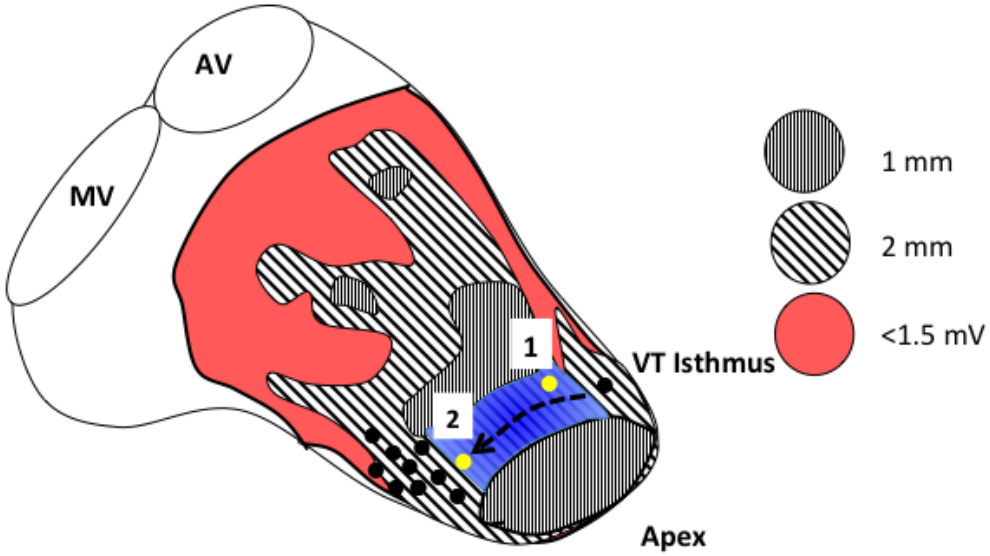

Figure 2: Schematic drawing of segments with different wall thickness and sites with matching pace-maps (back tags) and sites with concealed entrainment (yellow tags) in the same patient. At the yellow sites 1 and 2 entrainment mapping is performed during VT (Figure 3) in the same patient shown in Figure 1. Shown are mitral annulus, aortic valve and left ventricular apex.

Figure 3a

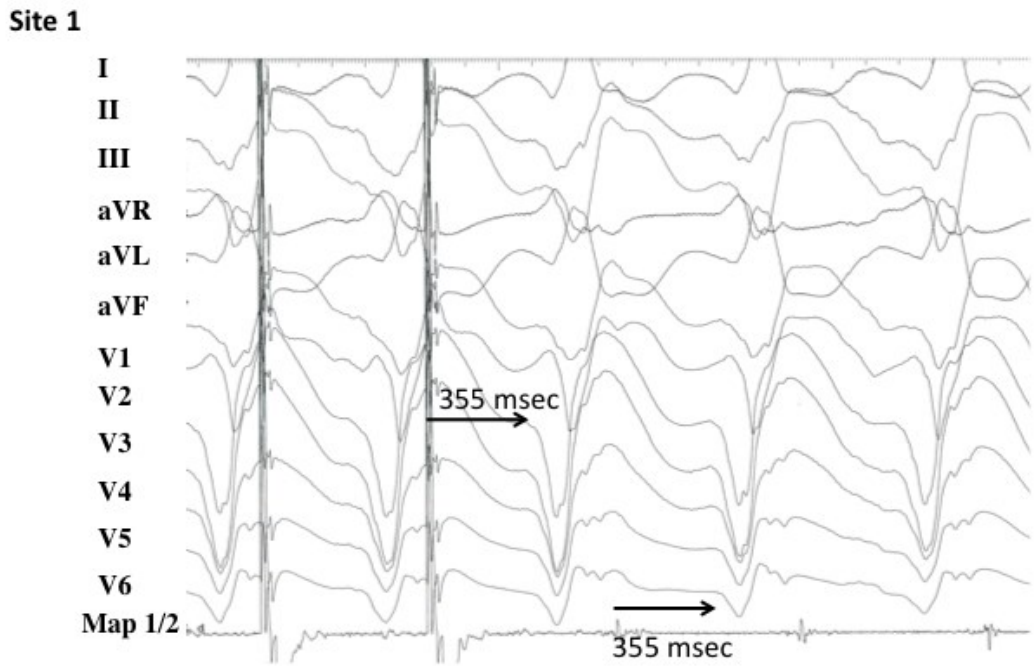

Figure 3a Pacing at site 1 shows a site with concealed entrainment and a long stimulus-QRS interval measuring 355 msec. This is close to the entry site of the reentry circuit. The stimulus-QRS interval matches the electrogram QRS interval. VT terminated when ablation was delivered at this location. However VT was still inducible with an increase in cycle length from 550 to 590 msec.

Figure 3b

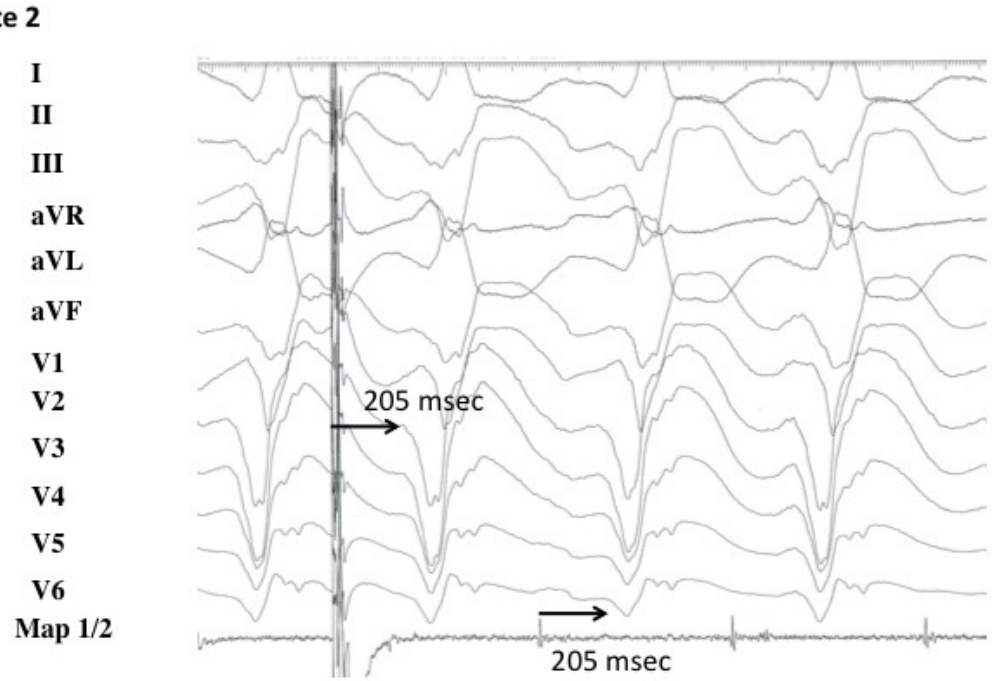

Figure 3b: Pacing at site 1 is closer to the VT exit and the stimulus-QRS interval of the last paced beat is 205 msec. This matches the electrogram-QRS interval. There were however changing stimulus-QRS intervals present at this site. VT terminated permanently and was no longer inducible after this ablation lesion was delivered.

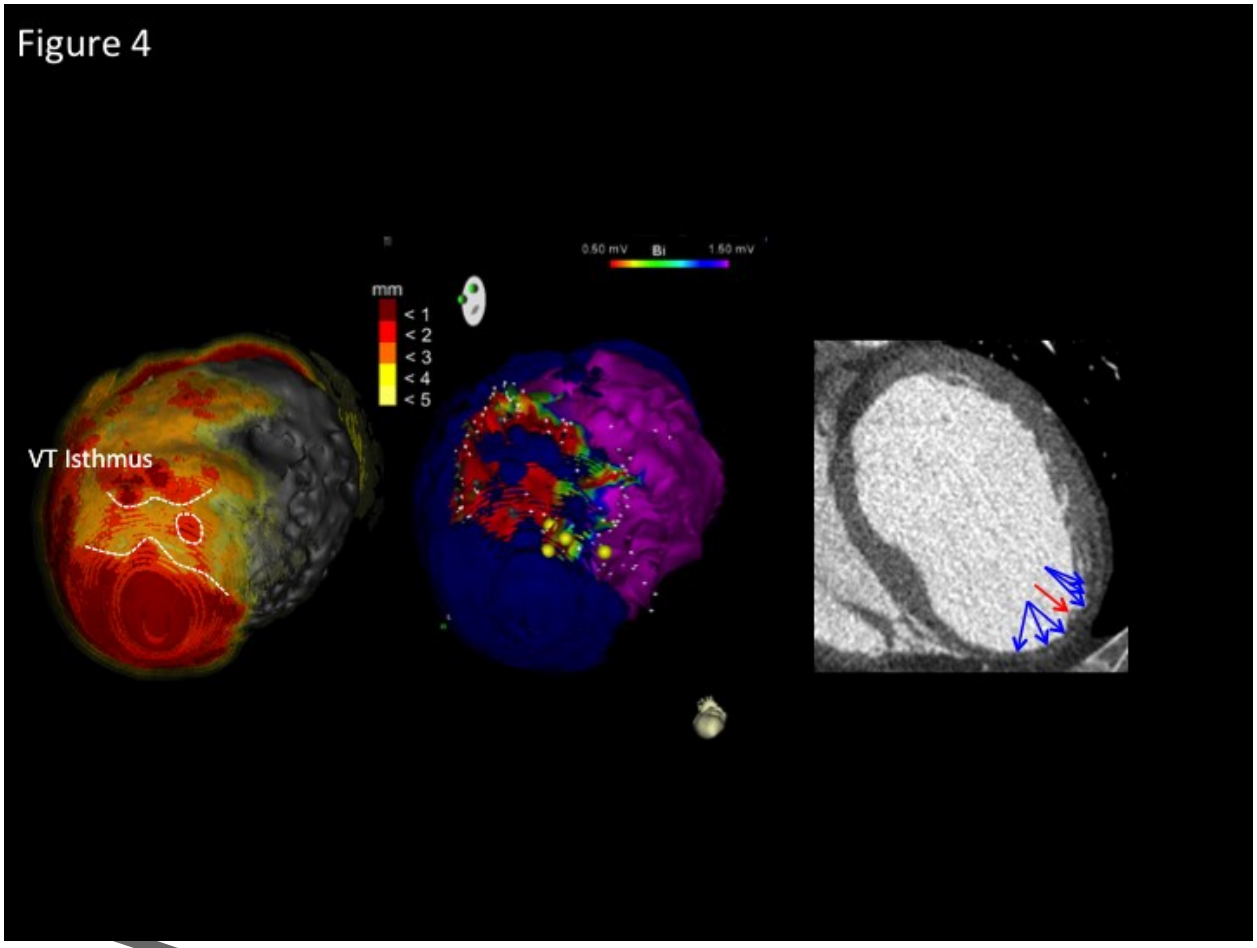

Figure 4: Left panel: Wall thickness defined by CT showing the location of a VT isthmus. Middle panel: Wall thickness of CT-defined scar (blue) ≤2 mm registered to eletroanatomic map. Target sites are indicated with yellow tags. Right panel: Axial view of CT illustrating the isthmus area where a ridge (red arrow) is located between 2 areas of wall thinning (blue arrows).